pentane was removed by fractional distillation. The residue was subjected to flash distillation under reduced pressure; all volatiles were collected in a dry ice cooled receiver. The volatile products were purified by preparative gas chromatography. All yields reported are isolated yields of purified products.

Without Solvent. Freshly sublimed potassium *tert*-butoxide (100% excess) was placed in a flask equipped with a condenser, a drying tube, an Ar inlet tube, and a septum cap. The butoxide was heated to an oil-bath temperature of 100 °C and then the labeled vinyl bromide was injected beneath the surface of the base via a syringe. The mixture was maintained at 100 °C for 10 min, cooled, and water was added to it. The water was extracted with pentane, and the pentane layers were washed with water and dried over $MgSO_4$. The pentane was removed by fractional distillation, and the residue was flash distilled under reduced pressure; all volatiles were collected in a dry ice cooled receiver and were purified by preparative gas chromatography. All reported yields are isolated yields of purified products.

Rearrangement Products. 1-Bromocyclopentene (10):[27] IR ($CHCl_3$) 2270, 2855, 1620, 1440, 1315, 1040, 1010, 945, 900 cm^{-1}; ^1H NMR (250 MHz) δ 5.84 (1 H, m), 2.57 (2 H, m), 2.30 (2 H, m), 1.98 (2 H, m); ^{13}C NMR δ 130.94 (C-2), 120.74 (C-1), 39.51 (C-5), 32.29 (C-3), 23.18 (C-4).

1-Bromo-4-ethoxy-5,5-dimethylcyclopentene (23): IR (neat) 2940, 2860, 1610, 1450, 1335, 1125, 1040, 990, 880, 815 cm^{-1}; ^1H NMR (60 MHz) δ 5.75 (1 H, t), 3.60 (3 H, m), 2.35 (2 H, dddd), 1.20 (3 H, t), 1.12 (3 H, s), 1.00 (3 H, s); ^{13}C NMR δ 132.20 (C-1), 125.39 (C-2), 85.44 (C-4), 65.48 (CH_2O), 49.58 (C-5), 36.23 (C-3), 26.09 (CH_3), 19.10 (CH_3), 15.40 (CH_3). Anal. Calcd for $C_9H_{15}BrO$: C, 49.32; H, 6.85. Found: C, 49.21; H, 6.95.

1-Bromo-4-ethoxy-3,3-dimethylcyclopentene (24): IR (neat) 2985, 2900, 1612, 1470, 1350, 1125, 1030, 845, 795 cm^{-1}; ^1H NMR (60 MHz) δ 5.75 (1 H, t), 3.58 (3 H, m), 2.70 (2 H, dddd), 1.20 (3 H, t), 1.10 (3 H, s), 1.00 (3 H, s); ^{13}C NMR δ 140.29 (C-2), 116.42 (C-1), 86.28 (C-4), 65.76 (CH_2O), 48.21 (C-3), 44.56 (C-5), 27.20 (CH_3), 20.66 (CH_3), 15.41 (CH_3). Anal. Calcd for $C_9H_{15}BrO$: C, 49.32; H, 6.85. Found: C, 49.21; H, 6.95.

1-Bromo-3,3,5,5-tetramethylcyclopentene (25): $bp_{2.5}$ = 31 °C; IR (neat) 3050, 2960, 1620, 1365, 1320, 850 cm^{-1}; ^1H NMR (60 MHz) δ 5.55 (1 H, s), 1.75 (2 H, s), 1.11 (6 H, s), 1.10 (6 H, s); ^{13}C NMR δ 138.75 (C-2), 131.29 (C-1), 52.65 (C-4), 48.19 (C-5), 43.54 (C-3), 30.25 (CH_3), 29.07 (CH_3); Anal. Calcd for $C_9H_{15}Br$: C, 53.22; H, 7.44. Found: C, 53.37; H, 7.65.

1-*tert*-Butoxy-3,3,5,5-tetramethylcyclopentene (26): IR 3100, 3000-2900, 1655, 1380, 1200, 1160; ^1H NMR (250 MHz) δ 4.28 (1 H, s), 1.50 (2 H, s), 1.31 (9 H, s), 1.06 (6 H, s), 1.03 (6 H, s); ^{13}C NMR δ 157.58 (C-1), 106.94 (C-2), 52.00, 44.89, 39.68, 32.13, 28.61, 27.93.

Treatment with 2,4-dinitrophenylhydrazine in ethanolic H_2SO_4 gave the 2,4-dinitrophenylhydrazone derivative of 2,2,4,4-tetramethylcyclopentanone, purified by TLC (4% ether/petroleum ether), mp = 146-148 °C; lit.[29] mp = 145-146 °C.

Incomplete Reaction of 1-(Bromomethylene-^{13}C)cyclobutane (9) with Potassium *tert*-Butoxide. A 200-mg sample of **9** (10% enriched) was subjected to the rearrangement reaction conditions at 36 °C in pentane. After 30 min, 35% rearrangement had occurred. The reaction mixture was worked up and unreacted **9** was recovered and was analyzed by ^{13}C NMR. All of the label was located on the bromomethylene carbon; no scrambling had occurred.

Reaction of 1-Bromo-3,3,5,5-tetramethylcyclopentene (25) with Potassium *tert*-Butoxide. A. In Pentane Solvent. A 150-mg sample of a 3.4/1.0 mixture of **25b**/**25a** was subjected to the rearrangement conditions for 3 h. Workup afforded a 72% recovery of **25** and no other volatile products. ^{13}C NMR analysis showed the ratio of **25b**/**25a** to be unchanged (3.4/1.0).

B. Without Solvent. A 460-mg sample of a 3.5/1.0 mixture of **25b**/**25a** was subjected to the rearrangement conditions for 10 min. Workup gave 76% recovered **25** as the only volatile product with the **25b**/**25a** ratio unchanged (3.5/1.00).

Acknowledgment. This work was supported in part by the National Science Foundation under Grant CHE-8408331. We acknowledge support of the Worcester Consortium NMR Facility at Clark University (NSF Grant No. DMR-8108697). We thank Dr. M. R. Brennan for assistance with the NMR experiments.

(29) Sandris, C.; Ourisson, G. *Bull. Soc. Chim. Fr.* **1956**, 958, 965.

Stereochemical Studies in Crystal Nucleation. Oriented Crystal Growth of Glycine at Interfaces Covered with Langmuir and Langmuir-Blodgett Films of Resolved α-Amino Acids§

E. M. Landau,† S. Grayer Wolf,† M. Levanon,† L. Leiserowitz,*,† M. Lahav,*,† and J. Sagiv*,‡

Contributions from the Departments of Structural Chemistry and Isotope Research, The Weizmann Institute of Science, Rehovot 76100, Israel. *Received June 16, 1988*

Abstract: In a stereochemical approach aimed at the understanding of crystal nucleation on a molecular level, the oriented crystallization of glycine at air-solution interfaces covered with monolayers **1-12** of resolved α-amino acids has been studied. Three types of monolayers with different packing motifs of the polar head groups have been used. Coverage of a supersaturated aqueous glycine solution with monolayers **1** and **2** did not lead to crystallization at the interface; on the other hand, coverage with monolayers **3-8** yielded a fast crystallization with only partial orientation. Finally, monolayers **9-12** yielded a fast nucleation of glycine with complete orientation of the crystals. These results imply that the packing of the polar head groups determines the nucleation rate and the degree of orientation of the attached growing crystals. This conclusion is strongly substantiated by the assignment of the structures of monolayers **3** and **9** using grazing-angle X-ray diffraction and reflectivity measurements from a synchrotron light source. Crystallization experiments were performed on solid hydrophobic glass supports coated with Langmuir-Blodgett films of monolayers of **1**, **3**, **4**, **6**, **9**, and **11**; in all cases the results were similar to those observed with the corresponding Langmuir monolayers.

I. Introduction

Although crystal nucleation is central to many processes in the living and inanimate world, its understanding and control on a molecular level is still at a rudimentary stage. Fundamental questions, such as the number of molecules needed for the nucleus to cross the critical size and the role played by surfaces and the solvent or foreign additives present in solution in the promotion or inhibition of primary or secondary nucleation, require clarification.

Studies of crystal nucleation that are based on thermodynamic

§ Dedicated to the memory of Prof. D. Ginsburg.
† Department of Structural Chemistry.
‡ Department of Isotope Research.

0002-7863/89/1511-1436$01.50/0

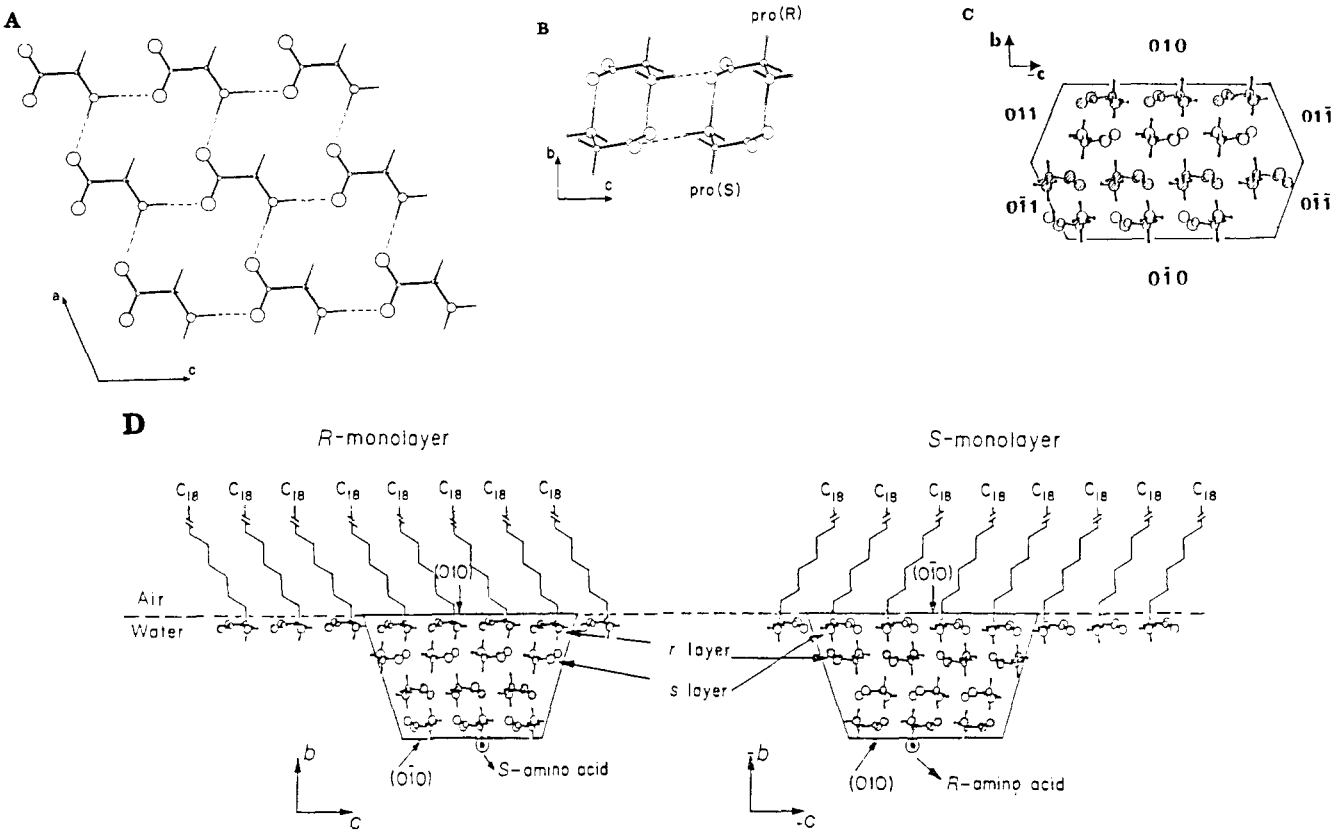

Figure 1. (A) An *ac* layer of hydrogen-bonded glycine molecules viewed along the *b* axis. The chiral layer is denoted as *r* since the H atoms of the C–H bonds that emerge from the *ac* plane are *pro-R*. (B) A centrosymmetric bilayer of hydrogen-bonded glycine molecules viewed perpendicular to the *bc* plane. The upper *r* layer is that shown in A. (C) Packing arrangement of α-glycine, delineated by its crystal faces. The bilayers (B) are related by 2-fold screw symmetry along the *b* axis. (D) Schematic views of pyramidal crystals of glycine grown under compressed α-amino acid monolayers of *R* and *S* absolute configuration. The (010) face is attached to the *R* monolayer and the (0$\bar{1}$0) face to the *S* monolayer. Amino acids of *S* and *R* absolute configuration are shown adsorbed from solution at the (0$\bar{1}$0) and (010) faces, respectively.

and kinetic data generally do not take into account the important molecular information available from the packing arrangement of the corresponding crystalline phase. In the present series of studies, we follow the hypothesis that the nucleus of a given crystalline phase assumes a structure akin to that of the mature phase. This approach has been instrumental in the past in the successful design of chiral polymers as enantioselective nucleation inhibitors in the resolution of racemic histidine into enantiomers,[1] as well as in the oriented growth of glycine crystals at interfaces in the presence of dissolved hydrophobic α-amino acids.[2] Here we shall describe a different approach based on the design of amphiphilic molecules forming floating Langmuir monolayers as artifical two-dimensional (2-D) nuclei for the promotion of crystal nucleation.[3] These molecules can be designed such that the hydrophilic head groups at the water interface constitute a surface that is identical with or complementary to a given layer at a given face of the to-be-grown single crystal. Furthermore, by changing substituents along the chain or diluting the monolayer with other amphiphiles it is possible to vary, albeit within limits, the packing arrangements of these head groups and the domain sizes of the films, thereby influencing the crystallization process in a controlled manner. Finally, the availability of new analytical tools such as surface X-ray diffraction from a synchrotron light source,[4] optical second harmonic generation,[5] and scanning tunneling microscopy[6] should enable the elucidation of the structure of such domains on a molecular level.

Following these lines of reasoning we chose to study the nucleation and crystal growth of α-glycine in aqueous solutions beneath floating Langmuir monolayers and solid-supported Langmuir–Blodgett films of optically resolved α-amino acids.

II. Modeling of the System

Glycine crystallizes from aqueous solution in the α-form (space group $P2_1/n$; a = 5.10, b = 12.0, c = 5.46 Å; β = 111.7°; Z = 4), exhibiting a bipyramidal habit.[7] The glycine molecules assume a chiral conformation in the crystal, in which the two hydrogens reside in different crystalline environments and are therefore diastereotopic. The glycine molecules, related by translation in the *ac* plane, form hydrogen-bonded chiral *ac* layers (Figure 1A). These glycine layers (designated as *r* and *s*), with a molecular cross-sectional area of 25.9 Å^2 (=$ac \sin \beta$), are juxtaposed on one side of the *b* axis by centers of inversion about which the molecules are interlinked by N–H···O bonds into dimers to form centrosymmetric hydrogen-bonded bilayers (Figure 1B). These layers are juxtaposed on the other side of the *b* axis by weak C–H···O and H···H contacts across the *n* glide plane, to complete the crystal structure (Figure 1C).

We may expect that the glycyl moieties of densely packed Langmuir monolayers of amphiphilic homochiral α-amino acid molecules would form a hydrogen-bonded layer arrangement very similar to that of glycine, provided the hydrophobic moieties of the monolayer allow their neighboring glycyl groups to be interlinked by N–H···O bonds. This is possible if the cross-sectional areas of the hydrophobic chains are equal to or smaller than the molecular *ac* cross-sectional area of α-glycine (25.9 Å^2). Consequently, a monolayer of resolved (*R*)-α-amino acids, in which

(1) Weissbuch, I.; Zbaida, D.; Addadi, L.; Leiserowitz, L.; Lahav, M. *J. Am. Chem. Soc.* **1987**, *109*, 1869.
(2) Weissbuch, I.; Addadi, L.; Leiserowitz, L.; Lahav, M. *J. Am. Chem. Soc.* **1988**, *110*, 561.
(3) Landau, E. M.; Levanon, M.; Leiserowitz, L.; Lahav, M.; Sagiv, J. *Nature* **1985**, *318*, 353.
(4) Als-Nielsen, J.; Pershan, P. S. *Nucl. Instrum. Methods* **1983**, *208*, 545.
(5) Rasing, Th.; Shen, Y. R.; Kim, M. W.; Valint, P., Jr.; Bock, J. *Phys. Rev.* **1985**, *A31*, 537.
(6) Binnig, G.; Rohrer, H. *Helv. Phys. Acta* **1982**, *55*, 726.
(7) Legros, J. P.; Kvick, A. *Acta Crystallogr.* **1980**, *B36*, 3052.

Table I. Crystallization of α-Glycine underneath Floating Langmuir Monolayers

	monolayer	limiting area/molecule, Å²	deg of orientatn, %	face preferent exposed to monolayer	crystallizn rate[a]
(*S*)-**1**	5-α-cholestan-3β-$OCOCH_2CH(NH_3^+)CO_2^-$	38	none		slow (h)
(*R*)-**2**	$(X)_2NCOCH_2CH(CO_2H)SCH_2CH(NH_3^+)CO_2^-$ ($X = CH_3(CH_2)_{14}COOCH_2CH_2^-$)	77			
(*S*)-**3**	$CF_3(CF_2)_9(CH_2)_2OCOCH_2CH(NH_3^+)CO_2^-$	30	50–79	(0$\bar{1}$0)	fast (s)
(*S*)-**4**	$CH_3(CH_2)_{14}CONH(CH_2)_3CH(NH_3^+)CO_2^-$	27	88–93	(0$\bar{1}$0)	fast (s)
(*R*)-**5**	$CH_3(CH_2)_{17}OCO(CH_2)_2CH(NH_3^+)CO_2^-$	29	73–97	(010)	fast (s)
(*S*)-**5**	$CH_3(CH_2)_{17}OCO(CH_2)_2CH(NH_3^+)CO_2^-$	29	73–93	(0$\bar{1}$0)	fast (s)
(*R*)-**6**	$CH_3(CH_2)_{15}CH(NH_3^+)CO_2^-$	25	85–96	(010)	fast (s)
(*S*)-**6**	$CH_3(CH_2)_{15}CH(NH_3^+)CO_2^-$	25	78–94	(0$\bar{1}$0)	fast (s)
(*R,S*)-**6**	$CH_3(CH_2)_{15}CH(NH_3^+)CO_2^-$	25	50	(010), (0$\bar{1}$0)	fast (s)
(*S*)-**7**	$CH_3(CH_2)_{17}NHCOCH_2CH(NH_3^+)CO_2^-$	27	39–77	(0$\bar{1}$0)	fast (s)
(*S*)-**8**	$CH_3(CH_2)_{17}NHCO(CH_2)_2CH(NH_3^+)CO_2^-$	27	51–96	(0$\bar{1}$0)	fast (s)
(*R*)-**9**	$CH_3(CH_2)_{14}CONH(CH_2)_4CH(NH_3^+)CO_2^-$	27	>99	(010)	fast (s)
(*S*)-**9**	$CH_3(CH_2)_{14}CONH(CH_2)_4CH(NH_3^+)CO_2^-$	27	>99	(0$\bar{1}$0)	fast (s)
(*R*)-**10**	$CH_3(CH_2)_{14}CONH(CH_2)_2CH(NH_3^+)CO_2^-$	27	>99	(010)	fast (s)
(*S*)-**10**	$CH_3(CH_2)_{14}CONH(CH_2)_2CH(NH_3^+)CO_2^-$	27	>99	(0$\bar{1}$0)	fast (s)
(*R*)-**11**	$CH_3(CH_2)_{17}OCOCH_2CH(NH_3^+)CO_2^-$	29	>99	(010)	fast (s)
(*S*)-**11**	$CH_3(CH_2)_{17}OCOCH_2CH(NH_3^+)CO_2^-$	29	>99	(0$\bar{1}$0)	fast (s)
(*S*)-**12**	$CH_3(CH_2)_{11}OCOCH_2CH(NH_3^+)CO_2^-$	29	>99	(0$\bar{1}$0)	fast (s)

[a] h, hours; s, seconds.

the polar head groups are packed as tightly as in an *ac* layer of glycine, should constitute a layer arrangement very similar to that of an *r* layer of glycine molecules exposed at the (010) face of the crystal (Figure 1A,B) and, thus, might induce nucleation of a glycine crystal with its (010) face attached to the monolayer. By symmetry, the corresponding monolayer of (*S*)-amino acids should induce nucleation of glycine with its (0$\bar{1}$0) face attached to the monolayer.

Controlled changes of the packing pattern of the glycyl head groups can be accomplished by insertion of bulky groups at various sites along the hydrophobic chains. Slight changes in the packing of the polar head groups should affect both the rate of nucleation and the degree of orientation of the growing crystals. Furthermore, when α-amino acids with bulky hydrophobic moieties such as steroids are used, upon compression such moieties will prevent the polar head groups from close packing, and thus the films might not serve as nucleators.

With these ideas in mind we synthesized three classes of amphiphilic resolved α-amino acids for the experiments on the crystallization of glycine.

III. Results

Crystallization of Glycine under Compressed Langmuir Monolayers of α-Amino Acids. Glycine was crystallized from supersaturated aqueous solutions under monolayers of three different types of resolved α-amino acids. Class i, to which **1** and **2** belong (Table I), is comprised of molecules in which the hydrophobic tail has a cross-sectional area larger than that of the polar head groups. Class ii is represented by the amino acid **3**, in which the hydrophobic tail is partially fluorinated. Class iii contains molecules **4**–**12**, in which the cross-sectional areas of the hydrophobic tails are equal to or smaller than that of the hydrophilic glycyl groups. For molecules of the first two but not of the third class, the glycyl groups are prevented from forming a hydrogen-bonded layer as in α-glycine.

When films of molecules **1** and **2**, which have a limiting molecular surface area (as measured over pure water) of 38 and 77 Å², respectively, were compressed over supersaturated solutions of glycine, no crystallization of glycine at the monolayer–water interface was noticed. In the few cases in which crystallization did occur, it started preferentially inside the aqueous solution and only later took place at the monolayer–solution interface.[8] In these cases the attached crystals displayed the normal bipyramidal habit and were randomly oriented vis-à-vis the monolayer.

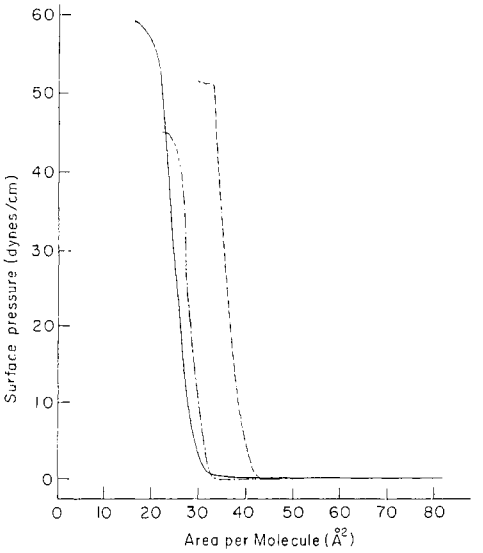

Figure 2. π–a diagrams of monolayers **1** (– –), **3** (–·–), and **11** (—) over H_2O at 20 °C.

In contrast, films of amphiphile **3**, with a smaller limiting molecular area of 30 Å², as determined by the π–a diagram (Figure 2), induced fast nucleation of glycine upon compression over supersaturated solution. Crystals assuming a pyramidal morphology appeared at the monolayer–water interface, with either the (010) or (0$\bar{1}$0) basal face attached to the monolayer. (We shall refer to crystals attached by their (010) or (0$\bar{1}$0) faces to the monolayer as "(010) oriented" or "(0$\bar{1}$0) oriented", respectively.) The orientation of the crystals vis-à-vis the monolayer was analyzed by several techniques: morphological observations, X-ray diffraction measurements (to determine the Miller indices of the faces attached to the monolayer), HPLC analysis of enantioselectively occluded chiral resolved α-amino acid additives and enantioselective dyeing with N^{ϵ}-(2,4-dinitrophenyl)-(*S*)-lysine. The details of these methods have been described previously.[2] When such a monolayer comprising molecules of *R* configuration was used, most of the glycine crystals were (010) oriented, and by symmetry, when a monolayer of *S* configuration was used, the (0$\bar{1}$0) oriented crystals were predominant. The degree of orientation induced by a monolayer of **3** in a large number of experiments ranged from 50 to 79% (see Table I).

Molecules of class iii display limiting molecular cross-sectional areas in the range of 25–29 Å². All these resolved monolayers,

(8) We have found that slight changes in experimental conditions such as supersaturation and temperature were of decisive influence with respect to appearance of crystals at the interface. Moreover, the use of diluted spreading solutions proved to enhance crystallization at interfaces, probably due to cooling of the interface.

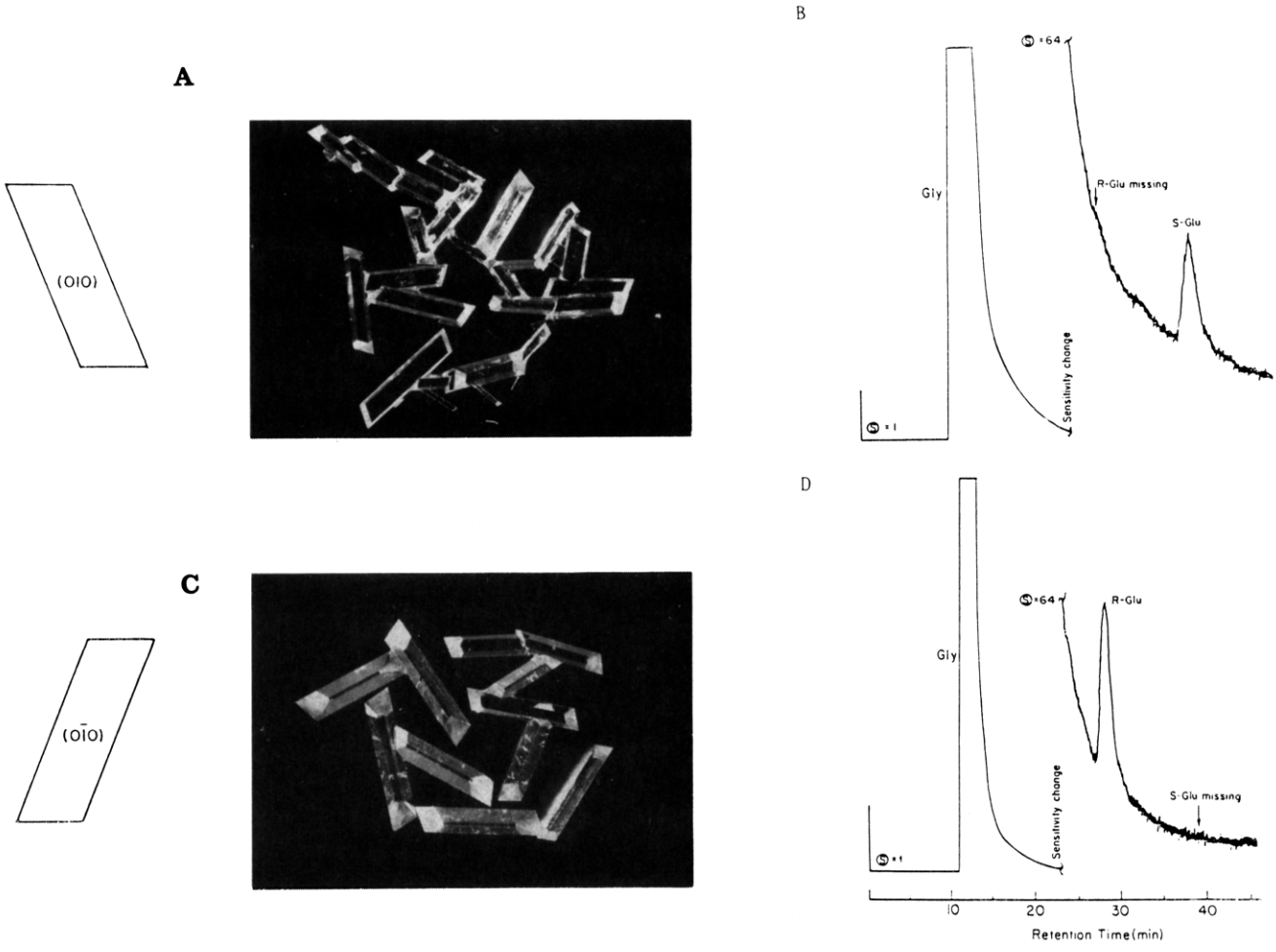

Figure 3. (A) A crust of glycine crystals grown under a monolayer of compound (*R*)-**11** in the presence of (*R,S*)-Glu. All the crystals are attached with their (010) faces to the monolayer and exhibit the same morphologies. One such crystal is schematically shown as a parallelogram viewed down the *b* axis. (B) HPLC analysis of an ensemble of crystals grown as in A, after washing with water, sensitivities as indicated. (C) A crust of glycine crystals grown under a monolayer of compound (*S*)-**11** in the presence of (*R,S*)-Glu. All the crystals are attached with their (0$\bar{1}$0) faces to the monolayer and exhibit enantiomorphous morphologies to those in A. One such crystal is schematically shown as a parallelogram viewed down the $-b$ axis. Note that it is not superimposable on the one depicted in A by rotation in the plane of the air–water interface. (D) HPLC analysis of an ensemble of crystals grown as in C, after washing with water, sensitivities as indicated.

when spread and compressed over supersaturated solutions of glycine, yielded fast nucleation of {010}[9] type crystals, albeit with various ratios of (010) to (0$\bar{1}$0) orientations. Four monolayers, palmitoyl lysine (**9**), γ-palmitoyl-α,γ-diaminobutyric acid (**10**), stearoyl aspartate (**11**), and lauroyl aspartate (**12**), caused fast nucleation with complete orientation of the glycine crystals. When monolayers of *R* configuration were used, all the crystals were (010) oriented, and by virtue of symmetry, when the *S* monolayers were used, the crystals were (0$\bar{1}$0) oriented. This completeness is demonstrated for a crust of oriented glycine crystals grown under a monolayer of **11** from a supersaturated solution containing 1% (*R*/*S*) glutamic acid (Figure 3). When the *R* monolayer was used, the glycine crystals exposed their (0$\bar{1}$0) face to the aqueous solution and thus occluded the (*S*)-glutamic acid only, and when the *S* monolayer was used, the glycine crystals exposed their (010) face to the aqueous solution and occluded the (*R*)-glutamic acid exclusively. Similar studies were conducted in the presence of minute amounts of N^{ϵ}-(2,4-dinitrophenyl)-(*S*)-lysine. Glycine crystals grown underneath the *R* monolayer appeared as yellow plates at the interface. On the other hand, the usual colorless pyramids crystallized when the *S* monolayers were used.

Similar experiments conducted with resolved monolayers of palmitoylornithine (**4**) and stearoyl glutamate (**5**) resulted in fast crystallization; the degree of orientation was however lower, 88–93% for **4** and 73–97% for **5**. In this respect we would like to mention that in a previous publication[3] we erroneously reported complete orientation for monolayer of compound **5**. Monolayers of α-aminostearic acid (**6**) yielded fast crystallization with an orientation of 78–96%. In contrast to all other compounds, the optical purity of this material could not be determined with precision higher than 95% by HPLC. We thus cannot say whether the lack of complete orientation is due to the structure or to the lower optical purity of the monolayer. A monolayer of **7**, (*S*)-aspartic acid–β-stearoylamide, with a surface area identical with that of stearoyl aspartate or lauroyl aspartate, led to slower crystallization with appearance of (010) and (0$\bar{1}$0) oriented crystals as well as some nonoriented bipyramidal ones. Of the (010) and (0$\bar{1}$0) oriented crystals, 39–77% were oriented in the expected sense. When a resolved monolayer of (*S*)-glutamic acid–γ-stearoylamide (**8**) was used, similar results were obtained, albeit with the somewhat higher degree of orientation of 51–96%.

Table II. Crystallization of α-Glycine at Langmuir–Blodgett Monolayers

mono-layer	deg of orientn, %	face preferent exposed to monolayer	mono-layer	deg of orientn, %	face preferent exposed to monolayer
(*S*)-**1**		none	(*R*)-**9**	>99	(010)
(*S*)-**3**	66–87	(0$\bar{1}$0)	(*S*)-**9**	>99	(0$\bar{1}$0)
(*S*)-**4**	55–95	(0$\bar{1}$0)	(*R*)-**11**	>99	(010)
(*R*)-**6**	80–97	(010)	(*S*)-**11**	>99	(0$\bar{1}$0)
(*S*)-**6**	90–96	(0$\bar{1}$0)			

Crystallization of Glycine on Langmuir–Blodgett (LB) Films. Oriented crystallization of glycine on LB films has also been tested;

(9) {010} denotes either (010) or (0$\bar{1}$0).

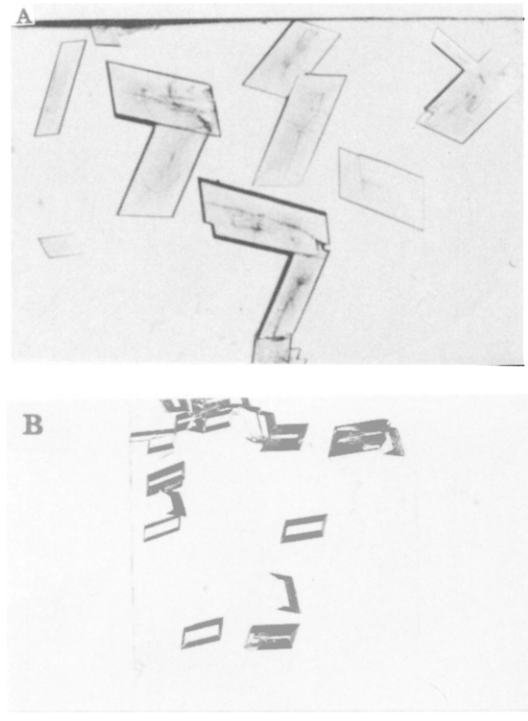

Figure 4. (A) Crystals of glycine grown on a LB film of (*R*)-**9** in the presence N^{ϵ}-(2,4-dinitrophenyl)-(*S*)-lysine. All the crystals appear as yellow plates attached with their (010) faces to the monolayer. (B) Crystals of glycine grown on a LB film of (*S*)-**9** in the presence N^{ϵ}-(2,4-dinitrophenyl)-(*S*)-lysine. All the crystals appear as transparent pyramids attached with their (0$\bar{1}$0) faces to the monolayer.

Table III. Crystallization of α-Glycine at Langmuir–Blodgett Multilayers

multilayer	no. of layers	outer layer	deg of orientatn, %	face preferent exposed to monolayer
(*S*)-**11**	6	(*R*)-**11**	>99	(010)
(*S*)-**11**	2	(*R*)-**11**	>99	(010)
(*R*)-**11**	6	(*S*)-**9**	>99	(0$\bar{1}$0)
(*R*)-**11**	2	(*S*)-**9**	>99	(0$\bar{1}$0)

these films were prepared by transferring the monolayer from the air–water interface onto a solid support. In order to fabricate LB films exposing the head groups away from the substrate, one must dip a hydrophobic substrate down through the monolayer. The standard substrate used was a glass slide rendered hydrophobic by its reaction with octadecyltrichlorosilane (OTS).[10] Table II summarizes the experimental results. Crystallization experiments performed with the various deposited monolayers give results very similar to those obtained with the floating ones. However, there are some differences. Crystallizations at the LB films were not as reproducible as those at the Langmuir films. One of the marked differences between the Langmuir and the LB regimes is the case of monolayer of **1**, which does not nucleate glycine at the air–water interface, but does so in the LB case, albeit without any orienting effect. Another pronounced difference between these regimes is exhibited by the morphologies of the basal {010} faces, in terms of the relative lengths of the edges that delineate the faces along the *a* and the *c* axes. Monolayers exhibiting complete orientation of the crystals were found to influence the attached {010} faces in such a way that the edge along the *a* axis is longer than that along *c* when spread at the air–water interface, while the opposite behavior was observed for these monolayers deposited as LB films (edge parallel to *c* longer than that along *a*), which is the normal morphology of the {010} face (Figure 4).

In order to confirm that only the outer monolayer of the LB films is responsible for the induced nucleation process, Y-type

(10) Maoz, R.; Sagiv, J. *J. Colloid Interface Sci.* **1984**, *100*, 465.

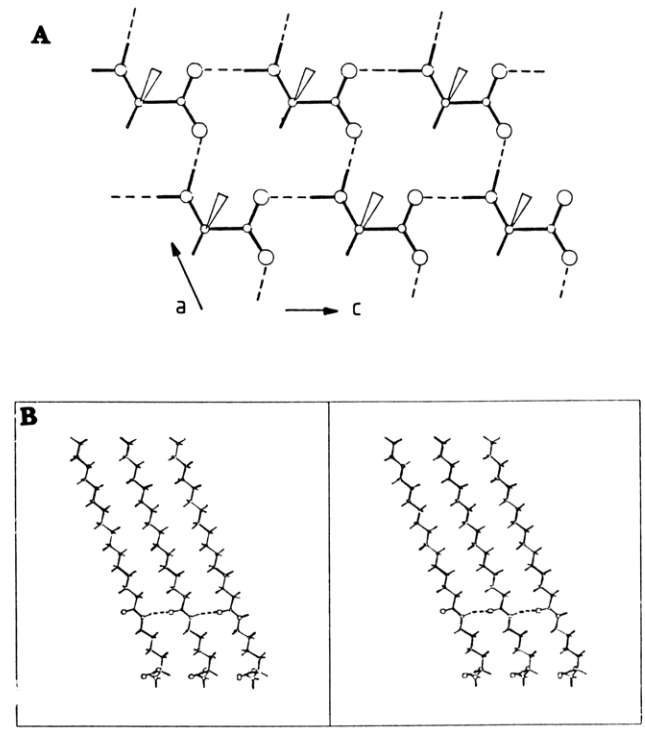

Figure 5. (A) Packing arrangement of palmitoyl-(*R*)-lysine (compound **9**) viewed perpendicular to the monolayer. The side chains are represented by wedges. (B) Stereoscopic view along the $a - c$ direction of a row of molecules parallel to the $a + c$ direction. Hydrogen bonding of neighboring secondary amides is denoted by the dashes.

multilayers were fabricated, in which the outer layer was of a different nature than the underlying ones. Table III summarizes the preliminary results. It can be seen that the outer layer is in fact the only one responsible for the orientational effect.

IV. Discussion

Previous studies on the crystallization of glycine in the presence of dissolved α-amino acids have shown that the latter act as efficient nucleation and crystal growth *inhibitors*.[11] Here we demonstrate, in contradistinction, that when α-amino acids are immobilized at an interface, and the polar α-amino acid head groups assume a structure similar or almost identical to that of one of the layers at a given face of α-glycine, they *promote* oriented nucleation at both the air–water and solid–water interfaces from these faces. Three classes of amphiphilic molecules were used, whose nucleating and orienting behavior critically depend on their limiting molecular surface areas relative to glycine in the *ac* plane. Monolayers of **1** and **2**, having a molecular surface area higher than 38 Å^2, do not promote nucleation at the interface. In these monolayers the bulky hydrophobic tails prevent the α-amino acid head groups from forming two-dimensional hydrogen- bonded structures. The absence of crystallization suggests that isolated glycyl moieties are not sufficient for promoting crystallizations at these interfaces, and that cooperativity between these groups is needed for the crystal nucleation. Substrate surface irregularities appear to cause nonoriented nucleation of glycine, as is suggested by the nonoriented crystallization behavior on LB films of **1**.

On the other hand, experiments underneath monolayers of classes ii and iii promoted immediate nucleation of glycine crystals, albeit with varying degrees of orientation. The crystallization underneath floating monolayers of compounds **9**–**12** results in complete orientation of the crystals. Recently the structure of a floating monolayer of (*R*)–**9** was determined by grazing-angle X-ray diffraction and reflectivity measurements from a synchrotron light source.[12,13] The packing arrangement of this

(11) Addadi, L.; Berkovitch-Yellin, Z.; Weissbuch, I.; Lahav, M.; Leiserowitz, L. *Top. Stereochem.* **1986**, *16*, 1.

(12) Grayer Wolf, S.; Leiserowitz, L.; Lahav, M.; Deutsch, M.; Kjaer, K.; Als-Nielsen, J. *Nature* **1987**, *328*, 63.

Chart I. Schematic Representation of a Compressed Langmuir Monolayer of **9**: Favorable Intermolecular Hydrogen-Bonding Contacts

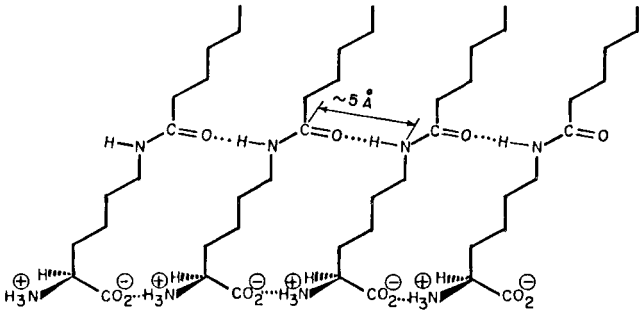

Chart II. Schematic Representation of a Compressed Langmuir Monolayer of **4**: Unfavorable Intermolecular Hydrogen-Bonding Contacts

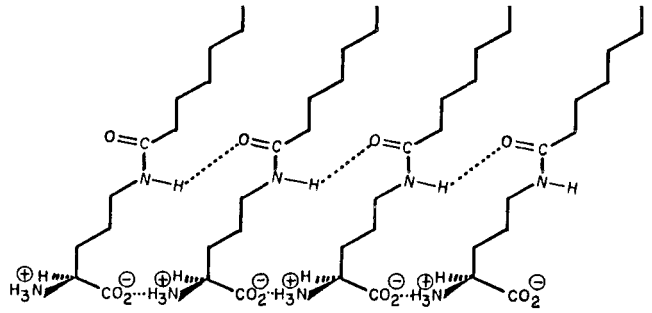

compressed monolayer is shown in Figure 5, and the arrangement of the glycyl moieties is almost identical with that of the *ac* layer of α-glycine molecules at the (010) face (Figure 1A). The side chains of the monolayer are inclined at 60° to the water surface, and the determined cell axes are a = 5.03 Å, c = 5.46 Å, and β = 117.8° ($ac \sin \beta$ = 24.3 Å^2). It is noteworthy that the molecular area of 24.3 Å^2 is ca. 10% less than 26.8 Å^2, which is the value determined from the X-ray reflectivity measurements. This was explained in terms of bare patches residing between 2-D monolayer domains of ca. 500 Å in diameter. The orientation of the glycyl moiety vis-à-vis the water surface is very similar to that of glycine vis-à-vis the *ac* plane of glycine crystal, i.e., the C(α)–C(β) bond is tilted from the plane to the same degree in both (*R*)-**9** and α-glycine, thus making it easy to appreciate the oriented crystallization. The amide groups, located at an even number of methylenes away from the α-carbon, allow the formation of an N–H···O bond along the (a + c) axis (Chart I). The repeat distance of 5.4 Å of the hydrogen bond along this axis is only 0.2 Å longer than the normal 5.2-Å translation distance between hydrogen-bonded amide groups. Analogously, the complete orientation underneath monolayer of **10**, having two methylenes between the amide group and the α-carbon, strongly suggests that the same packing arrangement of the head groups exists here. On the other hand, an odd number of methylenes between the α-carbon and the amide would necessitate a different orientation of the chains in order to obtain an N–H···O bond, presumably changing the packing arrangement of the polar head groups (Chart II). This appears to be the case of the monolayer of compound **4**. We denote this as an "odd/even" effect. The partial orientation of glycine crystals underneath this monolayer implies that the packing of the head groups is different from that of the lysine and the diaminobutyric acid homologues. Other evidence that this monolayer packs differently than **9** comes from preliminary surface diffraction studies, in which no diffraction peaks were observed.[14] Furthermore, the X-ray powder diffraction spectrum of crystalline **4** exhibits a very weak spectrum which is different from that of **9**. Moreover, the crystallization results with a monolayer of

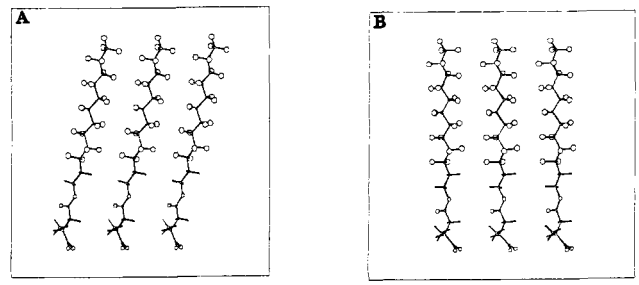

Figure 6. Models for the structure of a Langmuir monolayer of compound **3**. (A) Side view of the α-phase at surface pressures below 25 dyn/cm. (B) Side view of the β-phase at surface pressures above 25 dyn/cm.

Chart III. Schematic Representation of Compressed Langmuir Monolayers of **11**: and **12**: Favorable Interactions between Oxygen Lone Pairs and an Adjacent Methylene

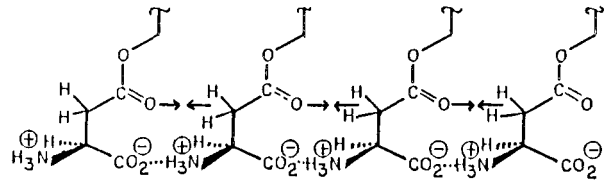

compound **7** support such an explanation. An N–H···O (amide) bond between molecules of **7** can only be achieved with a pronounced distortion of the molecular orientation and hence of the packing arrangement of the monolayer. On the other hand, we would have anticipated that a monolayer of **8** should behave like that of **9**, since the amide groups are located an even number of methylenes away from the α-carbon. However, the crystallization results show that monolayers of **8** induce a lower degree of orientation than the complete one exhibited by a monolayer of **9**. The explanation of this inconsistency must await the structural determination of the former monolayer. It is noteworthy that the complete orientation underneath both monolayers of **11** and of **12**, having the ester group at the same position along the chains but radically differing in their chain lengths, is a strong indication that the chain length plays only a minor role in determining the packing arrangement of the polar head groups.

Further, independent, evidence that a glycyl head group arrangement different from that of α-glycine may induce partial orientation of glycine crystals is provided by the determination of the packing arrangement of a m layer of the partially fluorinated compound **3**. According t n analysis of the grazing-angle diffraction and reflectivity me ements,[15] the structure undergoes a sharp solid–solid phase tr ition at approximately 25 dyn/cm involving a straightening of t side chains from a tilt of ca. 74° to 90° upon compression, and a concomitant transition from a distorted to a perfect hexagonal net (a = b = 5.82 Å, γ = 118.5° to a = b = 5.74 Å, γ = 120°). The packing arrangements of the molecules of these two phases are shown in Figure 6. Both structures differ from that of **9**, in terms of the inclination of the side chains of the molecules, and the lattice spacings. Since the packing arrangement of the glycyl moieties of **9** is similar to that of α-glycine, the orientation and arrangement of the glycyl head groups of the fluorinated monolayer **3** is radically different from that of α-glycine in the *ac* layer. This difference is reflected in the orientation induced. Interestingly, the degree of orientation of glycine crystals underneath monolayers of **3** was found to be pressure independent.

The differences in the degree of orientation between monolayers of compounds **11** and **5** (>99% vs 73–97%), in which the positions of the ester groups differ by one methylene only, can be explained by taking into consideration an analogous odd/even effect in the esters. If compressed molecules of **11**, having a β-aspartate head group, assume a molecular tilt of the chain similar to that of

(13) Grayer Wolf, S.; Kjaer, K.; Deutsch, M.; Landau, E. M.; Lahav, M.; Leiserowitz, L.; Als-Nielsen, J. *Thin Solid Films* **1988**, *159*, 29.
(14) This work is still in progress.
(15) Grayer Wolf, S.; Kjaer, K.; Deutsch, M.; Landau, E. M.; Lahav, M.; Leiserowitz, L.; Als-Nielsen, J. *Science* **1988**, *242*, 1286.

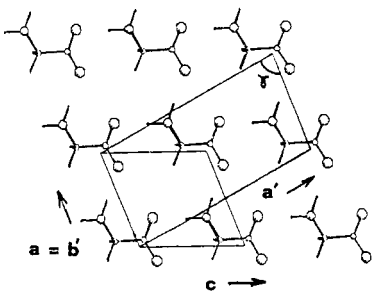

Figure 7. Transformation between the *ac* lattice of α-glycine and the centered *a'b'* lattices of the resolved hydrophobic amino acids. The angle between the *a* and (*a* + 2*c*) axes is 87° for α-glycine and 90° for the chiral resolved structures. See also ref 18.

palmitoyllysine (**9**), namely 60°, then we may envisage an arrangement exhibiting favorable C–H···O (carbonyl) and C–H···O (ether) interactions between neighboring molecules[16,17] (Chart III). On the other hand, for a similar tilt and arrangement for the compressed monolayer of **5**, having the γ-glutamate head group, the array would involve repulsion between oxygen lone pair electrons of adjacent molecules (Chart IV).

We have so far considered the growth of (010) oriented crystals underneath monolayers of (*R*)-α-amino acids and, by symmetry, (0$\bar{1}$0) oriented crystals underneath those of (*S*)-α-amino acids, as oriented crystallization via a pseudocenter of inversion. We shall now point out that nucleation of the (010) face by the (*S*)-α-amino acids and, by symmetry, the (0$\bar{1}$0) face by the (*R*)-α-amino acids may also be regarded as oriented nucleation. We shall describe two possible ways for achieving this orientation.

The first possibility is by formation of a pseudo 2-fold hydrogen-bonded bilayer between the Langmuir monolayer and the first glycine layer. In this respect we note that there are two ways of forming hydrogen-bonded bilayers of glycyl moieties. The layers may be related either by a center of inversion, incorporating centrosymmetric dimers as in layers r_1 and s_1 of α-glycine, or via a 2-fold axis.[18] The similarity between these two possibilities is shown in Figure 7. The crystal structures of resolved as well as racemic hydrophobic α-amino acids such as leucine, isoleucine, norleucine, and valine all form hydrogen-bonded bilayer structures,[19a] whose layer arrangements are all very similar to that of α-glycine. All the above racemic hydrophobic α-amino acids form bilayers via centers of inversion. Only the resolved compounds form bilayers generated by 2-fold symmetry due to the constraint of being chiral resolved. This result is compatible with a calculation according to which the centrosymmetric dimer is 5 kcal/mol more stable than the dimer generated by 2-fold symmetry.[19b] A direct manifestation of oriented crystal nucleation via pseudo 2-fold symmetry is provided by the fast nucleation of (*S*)-valine (Figure 8) with its {001} face under a compressed monolayer of (*S*)-**9**,

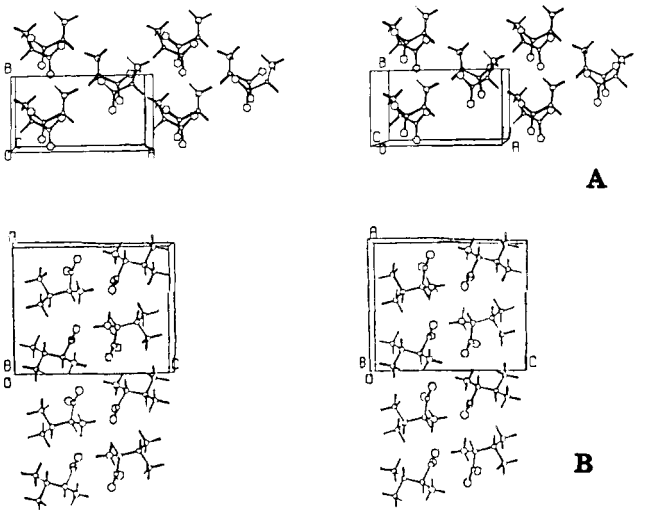

Figure 8. Packing arrangement of crystalline (*S*)-valine.[29] (A) Stereoscopic view down the *c* axis showing the hydrogen-bonded bilayer formed by 2-fold symmetry. There are 2 molecules per asymmetric unit cell, differing in the conformation of the side chains. For clarity, the side chains have been removed. (B) Stereoscopic view down the *b* axis showing the hydrogen-bonded bilayer formed by 2-fold rotation symmetry.

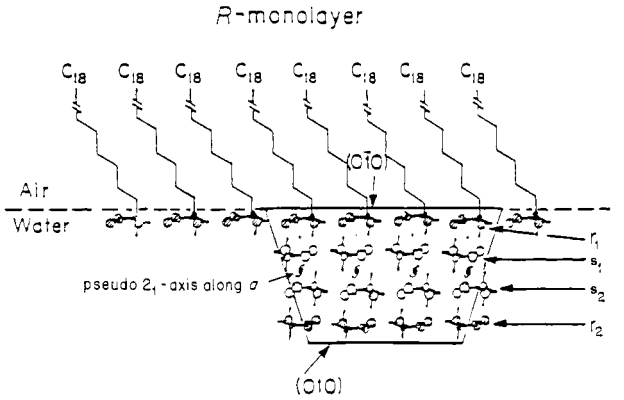

Figure 9. Schematic view of a pyramidal crystal of glycine attached with the (0$\bar{1}$0) crystal face to a compressed *R* amino acid monolayer.

which occurs at a similar rate to its nucleation under a compressed monolayer of (*R*)-**9**.[19b]

Although the pseudo 2-fold hydrogen-bonded bilayer is geometrically feasible, experimental and theoretical evidence is overwhelmingly in favor of a pseudocentrosymmetric bilayer involving the Langmuir monolayer and the first underlying glycine layer. Therefore, a more probable explanation for the appearance of oppositely oriented crystals, e.g., (0$\bar{1}$0) oriented crystals underneath a monolayer of *R* configuration, is provided by considering attachment of the s_2 glycine layer to the first pseudocentrosymetric bilayer via a pseudo 2-fold screw symmetry about the *a* axis (Figure 9). This layer is thus related to the s_1 layer above it by H···H and C–H···O contacts by 2-fold screw symmetry instead of by the *n* glide plane as in α-glycine (Figure 1C,D; see also Section II). This type of arrangement may occur in systems in which the packing of the head groups of the Langmuir monolayer is sufficiently different from the layer structure of α-glycine to introduce a distortion in the top layer of the attached crystal, so that the energy difference between bilayers related by pseudo 2-fold screw symmetry and those related by a glide is reduced.[20] One possible way to establish whether the 2-fold symmetry occurs across the N–H···O bond (i.e., between the monolayer and the first *ac* layer of glycine, or between the first and the second *ac* layers of glycine) may be by crystallization of meso di-α-amino

(16) Berkovitch-Yellin, Z.; Leiserowitz, L. *Acta Crystallogr.* **1984**, *B40*, 159.

(17) Taylor, R.; Kennard, O. *J. Am. Chem. Soc.* **1982**, *104*, 5063.

(18) Glycyl layers may form hydrogen-bonded bilayers via a pseudo 2-fold axis because the molecules are favorably arranged in a two-dimensional *ac* lattice which has a pseudo 2-fold axis parallel to *a*, i.e., the lattice is almost congruent with the same lattice rotated by 180° about the *a* axis. The similarity between the two-dimensional *ac* lattice of α-glycine and the *a'*,*b'* lattices of the resolved α-amino acids is provided by applying the transformation *a'* = (*a* + 2*c*), *b'* = *a* (see Figure 7). In α-glycine the angle between the *a* and (*a* +2*c*) axes is 87°, while in the chiral resolved structures the angle between the *a'* and the *b'* axes is 90° by symmetry. It is the smallness of this deviation, ~3°, that accounts for the nearly congruent relationship between these layers. Moreover, in α-glycine the length of *a* = 5.1 Å, *a* + 2*c* = 10.1 Å, whereas for example in resolved valine, *b'* = 5.3 Å, *a'* = 9.7 Å. We further note that the space groups of the resolved amino acids are either *C*2 (i.e., *ab* centered, containing a crystallographic 2-fold axis) or $P2_1$ with 2 molecules per asymmetric unit related by pseudo 2-fold symmetry, in keeping with the geometric constraint that the cell in these structures is pseudocentered and contains a pseudo 2-fold axis.

(19) (a) Di Blasio, B.; Pedone, C.; Sirigu, A. *Acta Crystallogr.* **1975**, *B31*, 601. Torii, K.; Iitaka, Y. *Acta Crystallogr.* **1973**, *B29*, 2799. (b) Grayer Wolf, S. M.Sc. Thesis, Feinberg Graduate School, Weizmann Institute of Science, 1986.

(20) In this context it is of interest to note that the crystal structure of racemic valine displays disorder across similar contacts.[19b]

Chart IV. Schematic Representation of a Compressed Langmuir Monolayer of **5**: Repulsion between Oxygen Lone Pairs of Adjacent Molecules

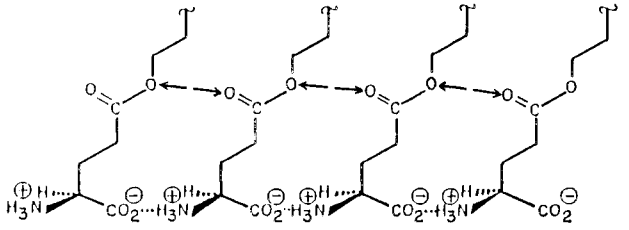

acids, provided they pack in a layer structure similar to that of α-glycine. If the disorder is induced by 2-fold rotation across the H···H contacts, then we expect complete oriented growth of the meso di-α-amino acids underneath monolayers such as **3** and **4**. We are currently searching for an appropriate crystalline system for such an experiment.

Experiments of the type described here might bear upon the important question of how many molecules with the correct orientation are needed in order to generate a nucleus of the critical size for crystal growth. Surface diffraction studies with a compressed monolayer of **9** suggest a domain size 500 Å in diameter, while similar studies with the fluorinated monolayer **3** suggest larger domains of at least 1500 Å. In order to furnish additional information on this point, we investigated the possibility of formation of structured domains at smaller compressions with monolayers of **9** and **11**. These crystallization experiments were performed at a variety of surface pressures and, therefore, of areas per molecule.[21] Under all conditions, a complete orientation of the crystals at the monolayer was observed, even up to surface areas 5 times the limiting values. These results suggest the spontaneous formation of aggregates whose structures are very similar to that of the compressed monolayer, but probably of much smaller size, which act as nucleation sites. The orientational effect is gradually lost at larger surface areas per molecule. Similar experiments conducted with monolayers of **1** and **3** at areas per molecule up to 5 times their limiting values showed no orientational effect. These observations seem to rule out a crystallization mechanism involving a trivial surface concentration effect. The present studies strongly suggest that the nucleation process involves organization of the nucleus at these structured domains and rules out a reciprocal mechanism, in which the nucleus of glycine, situated in the vicinity of the interface, may interact with poorly organized monolayer molecules to form the correct layer structure. In parallel studies, we are currently investigating the crystallization of glycine under mixed monolayers forming solid solutions. These systems might furnish information about the size of the smallest structured domain of α-amino acids needed for the initiation of the nucleation process.

The present approach might have some practical applications. The ability to coat solid surfaces with structured monolayers in a controlled manner might provide new nucleating surfaces for stereospecific and enantioselective separations by the process of crystallization. Moreover, this approach is not limited to organic crystals, but is also applicable to the crystallization of inorganic systems such as sodium chloride[22a] and calcium carbonate.[22b] The high degree of sensitivity of the crystallization method and the structural correlation between the packing arrangement of the polar head groups of the monolayer with the structure of the face attached to the monolayer suggests that, in the future, the crystallization method may become of considerable utility for the elucidation of the packing arrangement of surfaces.

Finally, the resolution of α-amino acids in solution, obtained by their occlusion into oriented crusts of glycine crystals attached to the monolayers, provides another route for the efficient amplification of optical activity on earth by crystallization, which we proposed recently.[2]

(21) Leveiller, F., private communication.
(22) (a) Landau, E. M.; Popovitz-Biro, R.; Levanon, M.; Leiserowitz, L.; Lahav, M.; Sagiv, J. *Mol. Cryst. Liq. Cryst.* **1986**, *134*, 323. Jacquemain, D., private communication. (b) Mann, S.; Heywood, B. R.; Rajam, S.; Birchall, J. D. *Nature* **1988**, *334*, 703.

Experimental Section

Monolayer Experiments. The materials used were as follows: hexane, $CHCl_3$ (Merck, spectroscopic grade), trifluoroacetic acid (TFA) (Merck, synthetic grade), H_2O (doubly distilled), glycine (BDH, >99%), (*R*,*S*)-glutamic acid (Fluka, puriss.), N^{ϵ}-(2,4-dinitrophenyl)-(*S*)-lysine (Sigma), (*S*)-valine (Fluka, analytical grade). All spreading solutions were prepared in hexane/TFA or $CHCl_3$/TFA in a v/v ratio of 96/4. π–a diagrams were measured with a thermostated circular trough equipped with a Wilhelmy balance (Mayer Feintechnik, Goettingen)[23] at 20 ± 2 °C over doubly distilled water. All crystallization experiments under Langmuir monolayers were carried out in the same type of trough by spreading and compressing the spreading solution over supersaturated aqueous solutions of glycine (4.66 M) or (*S*)-valine (0.6 M). Crystallization experiments on LB films were performed by dipping a glass slide, rendered hydrophobic by its reaction with OTS, through a compressed monolayer at 20 dyn/cm and 20 °C into a supersaturated aqueous solution of glycine (3.60 M). The crystals attached to the monolayer were isolated and analyzed for their orientation by chemical and crystallographic means as described previously.[2]

General Methods. Melting points (uncorrected) were determined on a Buchi apparatus. Infrared spectra were measured in KBr pellets (unless otherwise cited) on a FT infrared Nicolet MX-1 spectrometer and are given in cm^{-1}. ^1H NMR spectra were measured in deuterated TFA (unless otherwise cited) on a Varian FT-80A or Bruker WH-270 NMR spectrometers. All chemical shifts are reported (in δ) downfield from Me_4Si, and the *J* values are given in hertz. Splitting patterns are designated as follows: s, singlet; d, doublet; t, triplet; m, multiplet; br, broad. Optical rotations were measured by a Perkin-Elmer 141 polarimeter, using a 1-dm (1-mL) cell. Thin-layer chromatography (TLC) was performed on aluminum sheets precoated with silica gel (Merck, Kieselgel 60, F254, Art 5549). GC analyses for optical purity were performed on a Hewlett-packard 5890 gas chromatograph equipped with a Chirasil-(*S*)-valine column (25 m, i.d. 0.23 mm). HPLC analyses for optical purity were performed on a Waters liquid chromatograph equipped with a reversed C_{18} column, H_2O/ACN, 1/4.

Representative Procedure for the Syntheses of the β-Alkyl Esters of Aspartic (*R* and *S*) Acid (1, 3, 11, and 12) and the γ-Alkyl Esters of Glutamic (*R* and *S*) Acid (5). A solution of *N*,*N*′-dicyclohexylcarbodiimide (DCC, 1.1 mmol) in CH_2Cl_2 was added to a chilled solution of the *N*-carbobenzoxy-α*O*-benzyl amino acid (1 mmol), the corresponding alcohol (1.5 mmol), and 4-(dimethylamino)pyridine (0.2 mmol) in CH_2Cl_2 or THF. The reaction mixture was kept for $^1/_2$ h at 0 °C and subsequently for 2 h at 25 °C. The solution was refrigerated overnight, and precipitated dicyclohexylurea (DCU) was filtered off. The solution was washed with 0.5 N HCl, H_2O, $NaHCO_3$, and again with H_2O, dried over $CaCl_2$, and dried in vacuum. The residue was recrystallized from EtOH. The protected product was purified to one spot in TLC (benzene/dioxane/ether, 5/1/2). It was further hydrogenated for 2 h in H_2 atmosphere at room temperature in a solution of 90% TFA with catalytic amounts of Pd/C. The catalyst was filtered off and the solvent removed in vacuum. The residue was treated with acetonitrile (ACN) and MeOH to give a white powder, which was recrystallized from acetic acid and dried in vacuum for 24 h. All products gave one spot in TLC (propanol/ammonia, 7/3, ninhydrin development).

Procedure for the Synthesis of 2. *N*,*N*-Bis[2-(*n*-hexadecanoyloxycarbonyl)ethyl]maleamic acid[24] was reacted with L-cysteine according to a known procedure[25] to yield 65% of **2**.

Procedure for the Synthesis of 4. This compound was synthesized according to a known procedure.[26] The amounts used were as follows: active ester, 1.2 mmol; (*S*)-ornithine, 1.6 mmol; Et_3N, 2.5 mmol; acetone, 5 mL; H_2O, 5 mL. The reaction was carried out for 1 h in an ice bath.

Procedure for the Synthesis of Racemic α-Aminostearic Acid (6). **6** was prepared by aminolysis of α-bromostearic acid.

Procedure for the Resolution of 6. This was done according to a known procedure.[28] α-Aminostearic acid (18 g, 60 mmol) was refluxed in 30 g of formic acid (100%) for 8 h and cooled to 0 °C, and the precipitated crystals were filtered off and dissolved in ethyl acetate. After

(23) Fromherz, P. *Rev. Scient. Instrum.* **1975**, *46*, 1380.
(24) Tundo, P.; Kippenberger, D.; Politi, M. J.; Klahn, P.; Fendler, J. H. *J. Am. Chem. Soc.* **1984**, *104*, 5352.
(25) Neumann, R.; Ringsdorf, H. *J. Am. Chem. Soc.* **1986**, *108*, 487.
(26) Paquet, A. *Can. J. Chem.* **1976**, *54*, 733.
(27) Adamson, D. W. *J. Chem. Soc.* **1939**, 1564.
(28) Mills, A. K.; Wilder Smith, A. E. *Helv. Chim. Acta* **1960**, *43*, 1915.
(29) Torii, K.; Iitaka, Y. *Acta. Crystallogr.* **1970**, *B26*, 1317.

the nonreacted amino acid was filtered off, petroleum ether (40–60 °C) was added to the solution and the *N*-formylamino acid precipitated: yield 8.5 g (43%), mp 129 °C. This amount (26 mmol), dissolved in 200 mL of absolute EtOH, was added to a warm solution of brucine (10.25 g, 26 mmol) in 300 mL of absolute EtOH. The solution was refrigerated for 3 days, and the crystals of the (−)-(*R*)-brucine salt of the *N*-formylamino acid were filtered off and recrystallized twice from EtOH; 2 g thereof was dissolved in H_2O/EtOH, 30/1, and cooled to 0 °C. An excess of NH_3 was added and the mixture stirred for 2 h. The brucine was filtered off, and the solution was acidified with 6 N HCl and refrigereated overnight. The precipitated (−)-(*R*)-*N*-formyl-α-aminostearic acid was precipitated and recrystallized from EtOH: mp 114 °C, $[\alpha]_D = -26.9°$, EtOH. It was subsequently hydrolyzed by refluxing in 10% HCl for 2 h and neutralized with NH_4OH, and the amino acid separated. The more soluble diastereomeric brucine salt was treated in the same way to give the (+)-(*S*)-α-aminostearic acid.

Procedure for the Syntheses of 7 and 8. Dried *N*-hydroxysuccinimide (6 mmol) and DCC (6 mmol) in THF were added to *N*-carbobenzoxy-(*S*)-Asp-α-*O*-benzyl and *N*-carbobenzoxy-(*S*)-Glu-α-*O*-benzyl respectively (6 mmol, Bachem Feinchemikalien) in CH_2Cl_2. Moisture was excluded by a $CaCl_2$ tube. After being cooled for 5 min at 0 °C, stearoylamine (6 mmol) was added with stirring. The mixture was left overnight at room temperature. Precipitated DCU was filtered off (yields: 86 and 76.7% in the Asp and Glu syntheses, respectively). The filtrate was evaporated to dryness and recrystallized twice from MeOH. The protected product was purified to one spot in TLC (ethyl acetate/petroleum ether, 3/7 and 1/1, respectively): mp 103–105 °C, yield 2.26 g (67%); and mp 111–112 °C, 1.7 g (49%) for the Asp and Glu derivatives, respectively. A 0.5-g sample was treated with an excess of HBr/AcOH (45%) (BDH, GPR) and diluted to 30% with TFA at room temperature over $CaCl_2$. The excess reagent was removed by bubbling N_2. After the solvent was evaporated, the residue was trituated with ether, filtered off, and redissolved in MeOH. The product was reprecipitated by a dropwise addition of the solution to twice its volume of water, filtered off, washed with water, and dried. The products gave one spot in TLC (PrOH/NH_3, 7/3, ninhydrin development); the yield of **8** was 0.16 g (46%).

Procedure for the Synthesis of 9. This compound was synthesized according to a known procedure.[26]

Procedure for the Synthesis of 10. Compound **10** was synthesized by reacting palmitic acid succinimidyl ester with (*R*)- and (*S*)-αγ-diaminobutyric acid, respectively, according to a known procedure.[26] The reaction was carried out for 2 h in an ice bath and subsequently for 1 h at room temperature.

(*R*)- and (*S*)-αγ-diaminobutyric acid were synthesized according to a known procedure.[27]

The chemical purity of the compounds was established by elemental analysis, NMR, and IR spectroscopies.

Determination of the Enantiomeric Purity. Compounds 1–5 and 7–12. These compounds were hydrolyzed for 2 h in 6 N HCl at 100 °C., filtered through cotton wool, and evaporated to dryness with a stream of N_2. They were then derivatized by treatment with *i*-PrOH for 1 h at 100 °C, evaporated, treated with TFA/CH_2Cl_2, 1/4, at 0 °C for 20 min, dried, and redissolved in CH_2Cl_2. This solution was analyzed by GC.

Compound 6. A solution of DCC (1.1 mmol) and Et_3N (1.1 mmol) in THF was added to a solution of (+)- or (−)-*N*-formyl-α-aminostearic acid (1 mmol), (*S*)-phenylalanine hydrochloride methyl ester (1 mmol), and benzotriazole hydrate (1.2 mmol) in THF and kept overnight at 0 °C. The DCU was filtered off and the solution evaporated in vacuum; the residual diastereomeric dipeptide was dissolved in CH_2Cl_2 and washed with 0.1 N H_2SO_4 and $NaHCO_3$. The solution was dried over $CaCl_2$ and analyzed by HPLC.

Characterization of Compounds. Compound 1: mp 202 °C dec; $[\alpha]_D$ +27.73° (TFA); enantiomeric purity 99.3%; IR, 3450 (br), 2933, 2851, 1737, 1617, 1469, 1395 cm^{-1}; ^1H NMR (80 MHz) δ 0.63–2.4 (br m, 48 H), 3.43 (d, J = 4.4 Hz, 2 H), 4.75 (br t, 1 H), 4.82 (br m, 1 H). Anal. Calcd for $C_{31}H_{53}NO_5$: C, 73.91; H, 10.60. Found: C, 74.05; H, 10.53.

Compound 2: mp 70–72 °C; IR (Nujol) 1732, 1655, 1629 cm^{-1}; ^1H NMR (80 MHz, $CDCl_3$) δ 0.85 (t, J = 6.5 Hz, 6 H), 1.25 (br s, 52 H), 1.65 (m, 4 H), 2.10–3.85 (m, 9 H), 4.14–4.50 (m 5 H). Anal. Calcd for $C_{43}H_{80}N_2O_9S$: C, 64.50; H, 10.00; N, 3.50. Found: C, 63.95; H, 9.93; N, 3.33.

Compound 3. The esterification was performed in dioxane/THF: mp 196–197 °C dec; $[\alpha]_D$ +10.05°; enantiomeric purity 99.3%; IR, 3000 (br), 1738, 1604, 1519, 1414 cm^{-1}; ^1H NMR (80 MHz, TMS external) δ 2.6 (br m, 2 H), 3.49 (d, J = 5 Hz, 2 H), 4.7 (d, t, 3 H). Anal. Calcd for $C_{16}H_{10}F_{21}NO_4$: C, 28.29; H, 1.48. Found: C, 28.47; H, 1.76.

Compound 4: mp 238 °C dec; $[\alpha]_D$ +0.8° ($CHCl_3$/TFA); enantiomeric purity 98.33%; IR, 3298, 2918, 2850, 1636, 1585, 1558, 1415 cm^{-1}; ^1H NMR (80 MHz) δ 0.88–1.00 (m, 3 H), 1.20–2.50 (m, 30 H), 2.55–2.80 (m, 2 H), 3.50–3.70 (m, 2 H), 4.25–4.50 (m, 1 H). Anal. Calcd for $C_{21}H_{42}N_2O_3$: C, 68.06; H, 11.42; N, 7.56. Found: C, 68.36; H, 11.12; N, 7.62.

Compound (*S*)-5: mp 169 °C dec; $[\alpha]_D$ +6.85° (TFA); enantiomeric purity 99.8%; IR, 2919, 2850, 1729, 1582, 1520, 1472, 1451, 1412 cm^{-1}; ^1H NMR (80 MHz) δ 1.31 (br m, 37 H), 2.61 (br, t, 2 H), 2.86 (d, J = 4 Hz, 2 H), 4.27 (br t, 2 H), 4.53 (br t, 1 H). Anal. Calcd for $C_{23}H_{45}NO_4$: C, 69.13; H, 11.35. Found: C, 69.13; H, 11.21.

Compound (*R*)-5: mp 174 °C dec; $[\alpha]_D$ −7.1° (TFA); enantiomeric purity 100%; IR, identical with that of (*S*)-**5**; ^1H NMR (80 MHz) identical with that of (*S*)-**5**. Anal. Calcd for $C_{23}H_{45}NO_4$: C, 69.13; H, 11.35. Found: C, 69.20; H, 11.10.

Compound (*S*)-6: mp 232 °C; $[\alpha]_D$ +17.0° (TFA); enantiomeric purity 95.6%; IR, 3450 (br), 2920, 2850, 1700, 1471 cm^{-1}; ^1H NMR (80 MHz) δ 0.6–2.4 (br m, 33 H), 4.26–4.58 (br t, 1 H). Anal. Calcd for $C_{18}H_{37}NO_2$: C, 72.19; H, 12.45. Found: C, 72.30; H, 12.30.

Compound (*R*)-6: mp 232 °C; $[\alpha]_D$ −18.2° (TFA); enantiomeric purity 100%; IR, identical with that of (*S*)-**6**; ^1H NMR (80 MHz) identical with that of (*S*)-**6**. Anal. Calcd for $C_{18}H_{37}NO_2$: C, 72.19; H, 12.45. Found: C, 72.40; H, 12.70.

Compound 7: mp 227–229 °C; $[\alpha]_D$ +17.9° (TFA); enantiomeric purity 99.6%; IR, 3297, 2922, 2851, 1638, 1614, 1466 cm^{-1}. Anal. Calcd for $C_{22}H_{44}N_2O_3$: C, 68.70; H, 11.53; N, 7.28. Found: C, 71.26; H, 11.81; N, 7.51.

Compound 8: mp 215–220 °C dec; enantiomeric purity 99.7%; IR, 3337, 2918, 2850, 1643, 1603, 1529, 1467, 1412 cm^{-1}; ^1H NMR (80 MHz, CD_3OD) δ 0.89 (t, J = 7 Hz, 3 H), 1.28–1.50 (m, 32 H), 2.10–2.19 (m, 2 H), 2.47 (t, J = 7 Hz, 2 H), 3.17 (t, J = 7 Hz, 2 H), 4.01 (t, J = 7 Hz, 1 H). Anal. Calcd for $C_{23}H_{46}N_2O_3$: C, 69.30; H, 11.63; N, 7.03. Found: C, 70.15; H, 11.92; N, 7.31.

Compound (*S*)-9: mp 243–245 °C (AcOH); $[\alpha]_D$ + 9.7° ($CHCl_3$/TFA); enantiomeric purity 100%; IR, 3328, 2919, 2851, 1639, 1579, 1533, 1473, 1414 cm^{-1}; ^1H NMR (80 MHz) δ 0.88–1.00 (m, 3 H), 1.20–2.50 (m, 32 H), 2.55–2.80 (m, 2 H), 3.50–3.70 (m, 2 H), 4.25–4.50 (m, 1 H). Anal. Calcd for $C_{22}H_{44}N_2O_3$: C, 68.70; H, 11.53. Found: C, 68.71; H, 11.63.

Compound (*R*)-9: mp 243–245 °C (AcOH); $[\alpha]_D$ −11.5° ($CHCl_3$/TFA); enantiomeric purity 97.3%; IR, identical with that of (*S*)-**9**; ^1H NMR (80 MHz) identical with that of (*S*)-**9**. Anal. Calcd for $C_{22}H_{44}N_2O_3$: C, 68.70; H, 11.53; N, 7.28. Found: C, 68.39; H, 11.53; N, 6.97.

Compound (*S*)-10: mp 211–216 °C dec; enantiomeric purity 98.5%; IR, 3316, 2918, 2851, 1638, 1582, 1537, 1414 cm^{-1}; ^1H NMR (80 MHz) δ 1.00 (m, 3 H), 1.10–1.90 (m, 28 H), 2.00–2.10 (m, 2 H), 2.50–2.70 (m, 2 H), 3.80–3.90 (m, 1 H).

Compound (*R*)-10: mp 206–209 °C dec; enantiomeric purity 99.6%; IR, identical with that of (*S*)-**10**; ^1H NMR (80 MHz) identical with that of (*S*)-**10**.

Compound (*S*)-11: mp 204 °C dec; $[\alpha]_D$ +18.4° (TFA); enantiomeric purity 99.4%; IR, 3450 (br), 2919, 2851, 1730, 1585, 1472, 1416 cm^{-1}; ^1H NMR (80 MHz) δ 1.34 (br m, 35 H), 3.47 (d, J = 5 Hz, 2 H), 4.35 (t, J = 6.5, 2 H), 4.76 (t, J = 4.9 Hz, 1 H). Anal. Calcd for $C_{22}H_{43}NO_4$: C, 68.53; H, 11.24. Found: C, 68.40; H, 11.51.

Compound (*R*)-11: mp 200 °C dec; $[\alpha]_D$ −19.7° (TFA); enantiomeric purity 100%; IR, identical with that of (*S*)-**11**; ^1H NMR (80 MHz) identical with that of (*S*)-**11**. Anal. Calcd for $C_{22}H_{43}NO_4$: C, 68.53; H, 11.24. Found: C, 68.29; H, 11.10.

Compound 12: mp 207–209 °C dec; $[\alpha]_D$ +22.6° (TFA); enantiomeric purity 99.6%; IR, 3450 (br), 2919, 2852, 1731, 1585, 1417 cm^{-1}; ^1H NMR (80 MHz, TMS external) δ 1.4 (br m, 23 H), 3.47 (d, J = 5 Hz, 2 H), 4.34 (t, J = 6.5, 2 H), 4.70 (t, J = 5 Hz, 1 H). Anal. Calcd for $C_{16}H_{31}NO_4$: C, 63.76; H, 10.37. Found: C, 63.64; H, 10.07.

Acknowledgment. We thank Dr. K. Hill, E. Gati-Shavit, S. Conway, O. Blum, and Dr. D. Zbaida for help in the syntheses of the materials, Drs. K. Kjaer, J. Als-Nielsen, and M. Deutsch for cooperation in the X-ray experiments, R. Popovitz-Biro, L. Addadi, R. Maoz, and the late M. D. Cohen for stimulating discussions, and the donors of the Petroleum Research Fund, administered by the American Chemical Society, the U.S./Israel Binational Science Foundation, Jerusalem, and the Israeli Academy of Sciences and Humanities for financial support.

Registry No. (*S*)-**1**, 118355-78-5; (*R*)-**2**, 118355-79-6; (*S*)-**3**, 100578-14-1; (*S*)-**4**, 59012-45-2; (*R*)-**5**, 100578-13-0; (*S*)-**5**, 83789-61-1; (*R*)-**6**, 100680-17-9; (*S*)-**6**, 100680-18-0; (*R*,*S*)-**6**, 35289-39-5; (*S*)-**7**, 115574-03-3; (*S*)-**8**, 21291-46-3; (*R*)-**9**, 110578-78-4; (*S*)-**9**, 59012-43-0; (*R*)-**10**, 118355-80-9; (*S*)-**10**, 118355-81-0; (*R*)-**11**, 100578-12-9; (*S*)-**11**, 4582-80-3; (*S*)-**12**, 118375-51-2; H-Gly-OH, 56-40-6; Z-Asp-OCH_2Ph, 4779-31-1; Z-D-Asp-OCH_2Ph, 81440-35-9; Z-Glu-OCH_2Ph, 3705-42-8;

Z-D-Glu-OCH_2Ph, 65706-99-2; $F_3C(CF_2)_9CH_2CH_2OH$, 865-86-1; $Me(CH_2)_{17}OH$, 112-92-5; (Z)-$[Me(CH_2)_{14}CO_2CH_2CH_2]_2NCOCH{=}CHCO_2H$, 82797-95-3; H-Cys-OH, 52-90-4; $Me(CH_2)_{17}NH_2$, 124-30-1; (R)-$H_2NCH_2CH_2CH(NH_2)CO_2H$, 26908-94-1; (S)-$H_2NCH_2CH_2CH(NH_2)CO_2H$, 1758-80-1; $Me(CH_2)_{11}OH$, 112-53-8; Z-Asn-$[(CH_2)_{17}Me]OCH_2Ph$, 118355-82-1; Z-Gln$[(CH_2)_{17}Me]OCH_2Ph$, 118355-83-2; $Me(CH_2)_{15}CHBrCO_2H$, 142-94-9; 5α-cholestan-3β-ol, 80-97-7; palmitic acid succinimidyl ester, 14464-31-4.

Direct O-Acylation of Small Molecules Containing CO_2^----$H\ddot{N}$←HO Units by a Distorted Amide: Enhancement of Amine Basicity by a Pendant Carboxylate in a Serine Protease Mimic

K. I. Skorey, V. Somayaji, and R. S. Brown*

Contribution from the Department of Chemistry, University of Alberta, Edmonton, Alberta, Canada T6G 2G2. *Received June 27, 1988*

Abstract: The kinetics of the reaction of two series of amino alcohols (ethanol amines and 2-hydroxymethylimidazoles) with a distorted amide were studied as models for the acylation of the serine proteases. The pH/log k_2^{max} profiles plateau above the amine pK_a, indicating the basic form is active. In all cases, the reactions proceed by initial O-acylation to produce esters. With primary or secondary ethanolamines, subsequent O→N acyl transfer occurs to give amides. In each series, a Brønsted relationship exists relating the increasing amine pK_a with an increasing second-order rate constant for O-acylation. Amino alcohols containing a pendant carboxylate (e.g., serine and the 4(5)-[α,α-dimethylacetic acid] derivative of 2-hydroxymethylimidazole) fit on the Brønsted plots exactly, which suggests the amine pK_a controls the reactivity. The role of the carboxylate is to enhance the amine basicity by electrostatic/inductive means. This is particularly effective in solvents of reduced polarity (40% and 80% v/v, $EtOH/H_2O$) since the above effects counteract the normal drop in amine pK_a exhibited by the other amino alcohols that do not possess the CO_2^-. Both series exhibit low kinetic solvent isotope effects of between 1 and 2. In the imidazole alcohol series, as the amine pK_a increases the kinetic solvent isotope effect tends to 1.0. This is discussed in terms of a possible involvement of direct nucleophilic attack of an ammonium alkoxide zwitterion on **1**.

The serine proteases (SPases) comprise a large class of enzymes with active sites containing a $AspCO_2^-$---His imidazole---SerOH triad.[1] During the course of all SPase-catalyzed amide and ester hydrolyses, the SerOH group becomes transiently acylated. Although this suggests common hydrolytic pathways, continuing studies with various members of this class indicate subtle substrate-dependent diversities. For example, evidence exists that unnatural ester substrates such as phenyl benzoates[2a] and *p*-nitrophenyl acetate[2b] (pNPA) may be hydrolyzed by chymotrypsin via routes that involve first N-acylation of the His-57 imidazole followed by rapid acyl transfer to the Ser-195 hydroxyl. In addition, recent reports[3] using proton-inventory analysis indicate several SPases employ mechanisms that recruit 2 or more protons in flight for specific substrates and 1 proton in flight for nonspecific substrates.

Central to the issue of the function of the triad is the role of the $AspCO_2^-$ unit in influencing acylation of the SerOH. Two main possibilities have been discussed[4] at much length in the literature. These are stylized in Scheme I wherein the carboxylate acts either as a general base (path a) or to electrostatically enhance the imidazole basicity (path b). Recent evidence indicates that the $AspCO_2^-$---H^+-Im-His hydrogen bond is maintained in enzymes inhibited with species approximating the initial tetrahedral intermediate,[4,5] perhaps supporting path b. Even so, the issue has not been generally resolved, particularly since the proton inventory studies[3] leave open the possibility that the extent of involvement of the carboxylate may be substrate dependent. Nevertheless, the wide-spread occurrence of this catalytic triad suggests a considerable mechanistic advantage to the enzymes that employ it.

If such an arrangement leads to obvious acceleration, it is surprising how few studies have addressed the ability of a triad to facilitate O-acylation of a small molecule. A number of reports deal with the reaction of amino alcohols with esters[6] or reactive amides.[7] A smaller number deal with the interaction of imidazole and CO_2^- during acyl transfer from esters to H_2O,[8] although these

(1) For pertinent reviews of the structural and mechanistic properties of serine proteases see: (a) Walsh, C. *Enzymatic Reaction Mechanisms*; W. H. Freeman: San Fransisco, 1979; pp 56–97. (b) Fersht, A. *Enzyme Structure and Mechanism*; 2nd ed.; W. H. Freeman: San Fransisco, 1985. (c) Schowen, R. L. In Principles of Enzyme Activity; Liebman, J. F., Greenberg, A., Eds.; VCH Publishers Inc., Vol. 9, in press.

(2) (a) Hubbard, C. D.; Shoupe, T. S. *J. Biol. Chem.* **1977**, *252*, 1633. (b) Quinn, D. M.; Elrod, J. P.; Ardis, R.; Friesen, P.; Schowen, R. L. *J. Am. Chem. Soc.* **1980**, *102*, 5258.

(3) (a) Stein, R. L.; Strimpler, A. M. *J. Am. Chem. Soc.* **1987**, *109*, 4387. (b) Kovach, I. M.; Larson, M.; Schowen, R. L. *Ibid.* **1986**, *108*, 5490. (c) Stein, R. L.; Strimpler, A. M. *Biochemistry* **1987**, *26*, 2238. (d) Stein, R. L.; Strimpler, A. M.; Hori, H.; Powers, J. C. *Ibid.* **1987**, *26*, 1305.

(4) For summaries of the arguments in support of each possibility see ref 1c and: (a) Bachovchin, W. M. *Biochemistry* **1986**, *25*, 7751. (b) Abeles, R. H.; Liang, T.-C. *Ibid.* **1987**, *26*, 7603. (c) Bachovchin, W. M.; Roberts, J. D. *J. Am. Chem. Soc.* **1978**, *100*, 8041. (d) Satterthwait, A. C.; Jencks, W. P. *Ibid.* **1974**, *96*, 7018.

(5) Bone, R.; Shenvi, A. B.; Kettner, C. A.; Agard, D. A. *Biochemistry* **1987**, *26*, 7609.

(6) (a) Bruice, T. C.; Schmir, G. L. *J. Am. Chem. Soc.* **1958**, *80*, 148. (b) Werber, M. M.; Shalitin, Y. *Bioorg. Chem.* **1973**, *2*, 202. (c) Hine, J.; Khan, M. N. *J. Am. Chem. Soc.* **1977**, *99*, 3847. (d) Kitawa, Y.; Bender, M. L. *Bioorg. Chem.* **1975**, *4*, 237. (e) Kunitake, T.; Okahata, Y.; Sakamoto, T. *Chem. Lett.* **1975**, 459. (f) Sunamoto, J.; Kondo, H.; Okamoto, H.; Murakami, Y. *Tetrahedron Lett.* **1977**, 1329. (g) Hattori, K. *J. Inclusion Phenom.* **1984**, *2*, 669. (h) Moss, R. A.; Nahas, R. C.; Ramaswami, S. *J. Am. Chem. Soc.* **1977**, *99*, 627. (i) Fife, T. H.; Benjamin, B. *J. Chem. Soc., Chem. Commun.* **1974**, 525. (j) Bruice, T. C.; York, J. L. *J. Am. Chem. Soc.* **1961**, *83*, 1382. (k) Khan, M. N. *J. Org. Chem.* **1985**, *50*, 4851. (l) Anoardi, L.; Tonellato, U. *J. Chem. Soc., Chem. Commun.* **1977**, 401. (m) Kunitake, T.; Okahata, Y.; Tahara, T. *Bioorg. Chem.* **1976**, *5*, 155. (n) Tonellato, U. *J. Chem. Soc., Perkin Trans. 2* **1977**, 821. (o) Cram, D. J.; Lam, P. Y.-S.; Ho, S. P. *J. Am. Chem. Soc.* **1986**, *108*, 839. (p) Cram, D. J.; Katz, H. E.; Dicker, I. B. *J. Am. Chem. Soc.* **1984**, *106*, 4987.

(7) (a) Page, M. I.; Jencks, W. P. *J. Am. Chem. Soc.* **1972**, *94*, 8818. (b) Somayaji, V.; Skorey, K. I.; Brown, R. S.; Ball, R. G. *J. Org. Chem.* **1986**, *51*, 4866. (c) For a preliminary account of this work see: Somayaji, V.; Skorey, K. I.; Brown, R. S. *J. Am. Chem. Soc.* **1988**, *110*, 5205.

(8) (a) Komiyama, M.; Bender, M. L. *Bioorg. Chem.* **1977**, *6*, 13. (b) Komiyama, M.; Bender, M. L.; Utaka, M.; Takeda, A. *Proc. Natl. Acad. Sci. U.S.A.* **1977**, *74*, 2634. (c) Mallick, I. M.; D'Souza, V. T.; Yamaguchi, M.; Lee, J.; Chalabi, P.; Gadwood, R. C.; Bender, M. L. *J. Am. Chem. Soc.* **1984**, *106*, 7252. (d) Rogers, G. A.; Bruice, T. C. *Ibid.* **1974**, *96*, 2473. (e) Komiyama, M.; Breaux, E. J.; Bender, M. L. *Bioorg. Chem.* **1977**, *6*, 127. (f) Roberts, J. D.; Kanamori, K. *Proc. Natl. Acad. Sci. U.S.A.* **1980**, *77*, 3095.

0002-7863/89/1511-1445$01.50/0